

MECHANOLUMINESCENCE GLOW CURVE OF ZnS:Mn NANOCRYSTALS PREPARED BY CHEMICAL ROUTE

RAVI SHARMA^{a*}, D.P. BISEN^b, N. BRAHME^b, B.P. CHANDRA^c

^a*Department of Physics, Arts and Commerce Girls College, Raipur – 492001, India*

^b*School of Studies in Physics and Astrophysics, Pt. Ravishankar Shukla University, Raipur, (C.G.), 492010, India*

^c*Disha Academy of Research and Education, Disha Institute of Management and Technology, Satya Vihar, Vidhansabha-Chandrakhuri Marg, Raipur (C.G.) 492101, India*

This paper reports the synthesis of ZnS:Mn nanocrystals using chemical route; in which mercaptoethanol was used as the capping agent. The particle size of such nanocrystals was measured using XRD and TEM patterns and was found to be in between 3nm - 5nm. When a ZnS:Mn nanocrystal are deformed impulsively by applying a load from a fixed height, then initially the ML intensity increases with time, attains a peak value I_m at a particular time t_m , and later on it decreases with time. The peak intensity I_m increases linearly with the increasing height of the load. After t_m , initially the ML intensity decreases at a fast rate, and later on it decreases at a slow rate. The ML in ZnS:Mn nanocrystals can be understood on the basis of the piezoelectrically -induced electron detrapping model, in which the local piezoelectric field near the Mn^{2+} centres reduces the trap-depth, and therefore, the detrapping of filled electron traps takes place, and subsequently the energy released non-radiatively during the electron-hole recombination excites the Mn^{2+} centres and de-excitation gives rise to the ML.

(Received December 15, 2010; accepted February 22, 2011)

Keywords: Mechanoluminescence, Triboluminescence, Nanocrystals, XRD, TEM, Chemical route, ZnS:Mn

1. Introduction

Semiconductor nanocrystals are described as a state of matter that is intermediates between individual molecule and bulk [1]. Transition from bulk to nanoparticles lead to the display of quantum mechanical properties and an increased dominance of surface atoms which increases the chemical reactivity of a material. Notable examples include tunable bandgap [2] and catalytic behavior [3], respectively. The small size and high optical activity of certain semiconductors make them interesting for applications in disciplines ranging from optoelectronics [4], catalysis [5] to fluorescence microscopy [6].

Particles in nanometric sizes show unique physical properties, for example, with the decrease of particle size, extremely high surface area to volume ratio is obtained leading to an increase in surface specific active sites for chemical reactions and photon absorption to enhance the reaction and absorption efficiency. The enhanced surface area increases surface states, which changes the activity of electrons and holes, affecting the chemical reaction dynamics. For instance, the size quantization can increase the bandgap of photocatalysts to enhance the redox potential of conduction band electrons and valence band holes. Size dependent luminescence, enhance oscillator strength, non-linear optical effects, geometrical structure, chemical bonds, ionization

* Corresponding author: rvsharma65@gmail.com

potential, mechanical strength, melting point etc. are affected by particle size. Also, nanoparticles can induce the possibility of indirect electron transitions at the boundary of the crystals and realize the essential enhancement of light absorption.

The luminescence induced by any mechanical action on solids is known as mechanoluminescence (ML). The light emissions induced by the elastic deformation, plastic deformation, and fracture of solids are called elastico ML, plastico ML and fracto ML, respectively, and the light induced by rubbing of solids or separation of two solids in contact is known as tribo ML or triboluminescence. Many crystals are known to give electromagnetic radiation including electrons, ions, and photons during fracture [7–9] and some of them can even emit light during their deformation [10]. However, the radiation intensity in most materials is too weak and difficult to detect. Until now, a few academic studies concerning this physical phenomenon have been carried out in some crystals or minerals [11–15]. In the recent past the intense elastico and fracto mechanoluminescent materials have been found to have the potential for the stress sensor, fracture sensor, damage sensor, impact sensor, and for the visualizations of stress field near the crack-tip, stress distribution in the solids, and quasi-dynamic crack-propagation in solids [16,17-21]. Research on ML of ZnS:Mn nanocrystals prepared by chemical route in the powder form has not been reported to the best of our knowledge. This is the very first paper reporting it, and this will play an important role in both scientific and technological fields.

When a load is applied on to a solid, initially the ML intensity increases with time, attains a peak value and then it decreases with time. Such a curve between the ML intensity and deformation and post-deformation time of a solid is known as the ML glow curve. In this work zinc sulfide nanocrystals are prepared by chemical precipitation technique in which mercaptoethanol has been used for capping, which modifies surface of nanoparticles and prevents the growth of the particles to larger size. The ML glow curve of ZnS:Mn nanocrystals was studied, where the ML is induced by the impulsive deformation of the nanoparticles.

2. Experimental

The most important step in the studies of nanoparticles is their synthesis. There are various methods reported for synthesis of nanoparticles. Chemical route is used in the present investigation. The powder of ZnS nanoparticles were prepared by using chemical deposition technique described by Khosravi [22]. For synthesis, the 1M aqueous solution of ZnCl₂ and 1M aqueous solution of Na₂S were mixed in the presence of various concentrations of mercaptoethanol solution. MnCl₂ was also mixed in the solution in ratio 99:1, while stirring the solution continuously. The obtained precipitate was washed thoroughly three to four times in double distilled water and then separated by centrifuge at 3500 rpm, and finally air dried. Special care has to be taken to maintain the same physical condition during the synthesis of the sample.

The morphologies and sizes of the mercaptoethanol capped ZnS:Mn were determined by X-ray diffraction studies with Cu K α radiation ($\lambda=1.5418$ Å). XRD data were collected over the range 20⁰-70⁰ at room temperature. X-ray diffraction patterns have been obtained by Rigaku Rotating Anode (H-3R) diffractometer. The particle size was calculated using the Debye-Scherrer formula. Tecnai 20 G2 (FEI make) Transmission Electron Microscope was used to take the TEM photograph.

3. Mechanism of ml in ZnS:Mn nanocrystals

ZnS crystals are non-centrocentric [23], hence, the piezoelectrification caused by elastic deformation may give rise to the light emission [24-33]. The other possibility for the occurrence of ML in ZnS:Mn crystals may be the electrostatic interaction between charged dislocations and filled electrons traps [34,35], but its possibility in case of nanoparticles can be eliminated.

The mechanism of the ML in ZnS:Mn crystals may be understood in the following way :

(i) The deformation of ZnS:Mn crystals produces piezoelectric field because crystal – structure of ZnS is non-centrosymmetric .

(ii) Because of the decrease in the trap-depth due to the piezoelectric field, the detrapping of electrons from filled-electron traps takes place, and therefore, electrons reach the conduction band.

(iii) The electrons reaching the conduction band may recombine with the holes trapped in the defect centres or they may fall to the valence band and subsequently energy may be released non-radiatively.

(iv) The energy released non-radiatively during electron-hole recombination and falling of electrons from the conduction band to the valence band may be transferred to the Mn^{2+} ions, whereby Mn^{2+} ions may get excited [36-39].

(v) The de-excitation of excited Mn^{2+} ions gives rise to the light emission characteristic of the Mn^{2+} ions.

4. Results and discussion

The XRD patterns for the samples are shown in Fig. 1. Three different peaks are obtained at 2θ values of 29.50° , 48.80° and 57.80° . This shows that the samples have zinc blende structure and the peaks correspond to diffraction at (111), (220) and (311) planes, respectively [40]. The lattice parameter has been computed as 5.31 \AA , which is very close to the standard value (5.42 \AA). It is also seen from the figure 1 that peaks are broadened for higher concentration of capping agent. The broadening of peaks indicates nanocrystalline behavior of the particles. The size of the particles has been computed from the width of first peak using Debye Scherrer formula [41].

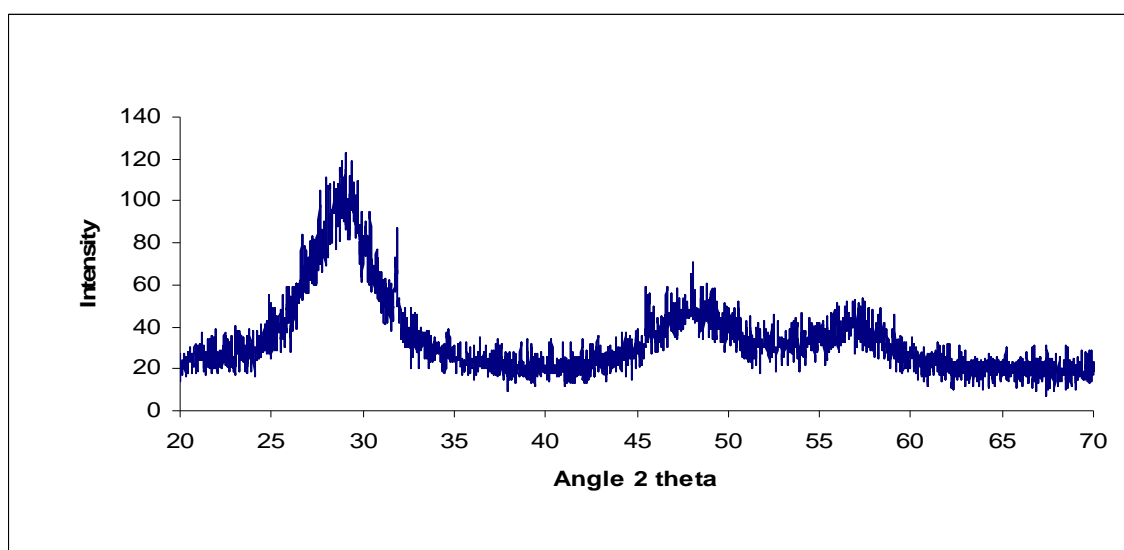


Fig. 1. XRD pattern of ZnS:Mn nanocrystal.

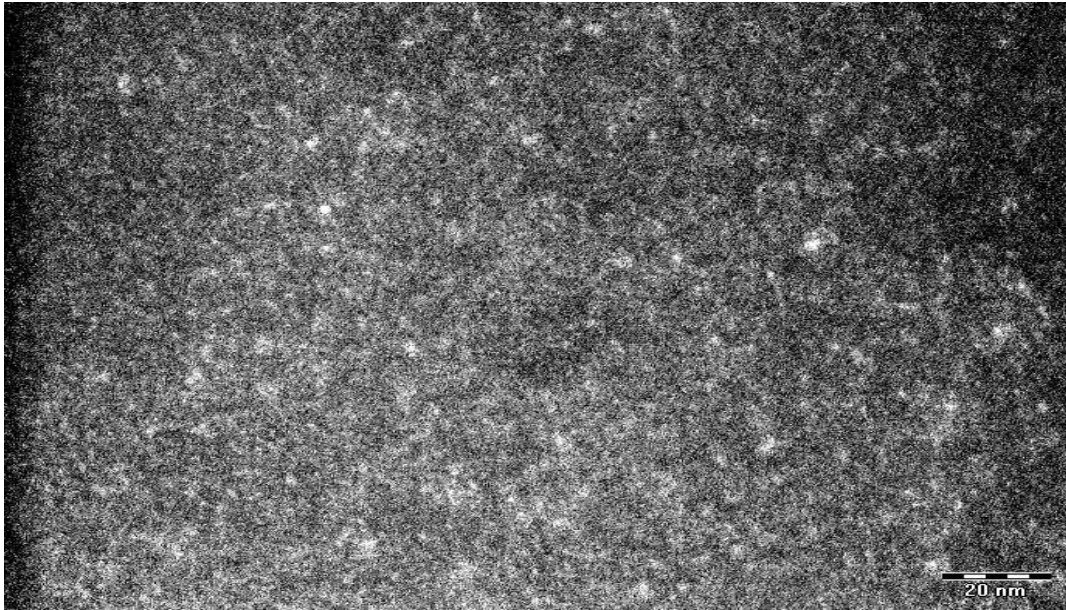


Fig.2 TEM photograph of ZnS:Mn nanocrystal.

A typical TEM image of ZnS nanoparticle is shown in Fig.2. The particle sizes obtained from TEM images are found to be in the range of 3nm to 5nm. TEM image shows clearly that the particles are not spherical.

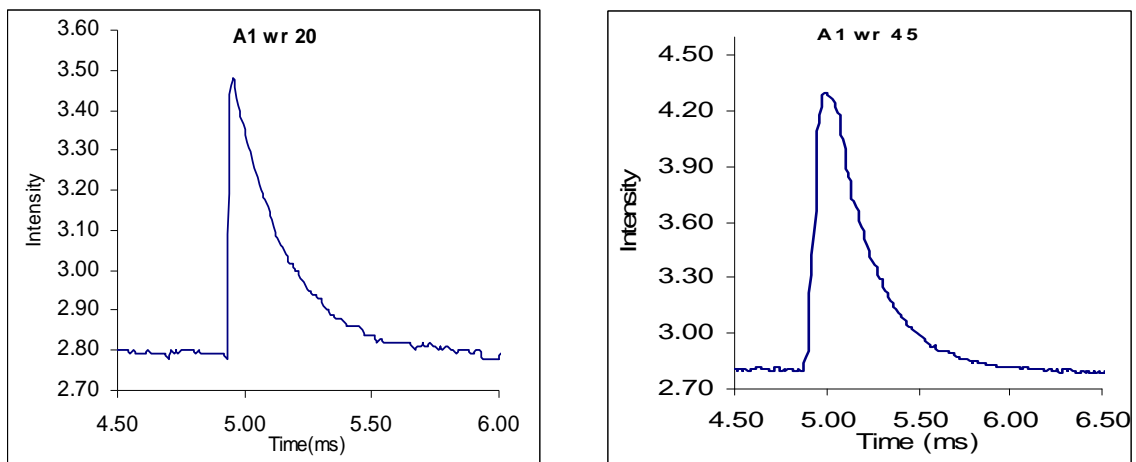


Fig.3(a) ML of ZnS:Mn nanocrystals dropping a load from 20 cm. 3(b) ML of ZnS:Mn nanocrystals obtained by obtained by dropping a load from 45 cm

Figure 3(a) and 3(b) shows the ML response to a mechanical impact. The fig. 3(a) shows ML curve of a sample of ZnS:Mn nanocrystale for the dropping height 20cm and 3(b) shows ML curve of the same sample for the dropping height 45cm. Note that the ML response transits of ZnS:Mn are similar to those of piezoelectric voltage responses, as reported previously [42]. The energy conversion efficiency for converting mechanical energy to photon energy, roughly estimated from the experimental data, is of the order of 10^{-6} . The ML intensity increases linearly with the increase of the falling height of the free cylinder; that is, the ML intensity increases with the increasing impact energy. These samples are not radiated by any of the source such as UV, Laser or γ radiation.

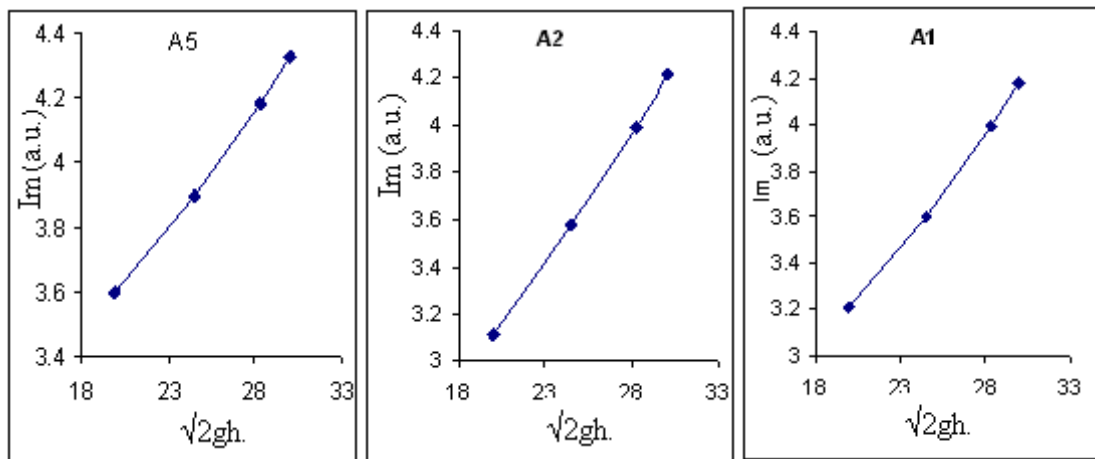


Fig.4 Dependence of ML on the falling height of three samples of ZnS:Mn nanocrystal.

Fig. 4 shows the plot between maximum ML intensity I_m and $\sqrt{2gh}$ of three different samples of ZnS:Mn; where h is having values 20, 30, 40 and 45 cm. The ML intensity of ZnS:Mn nanocrystal increases with increasing the mechanical stress. The intensity increases linearly with the increasing impact velocity $\sqrt{2gh}$.

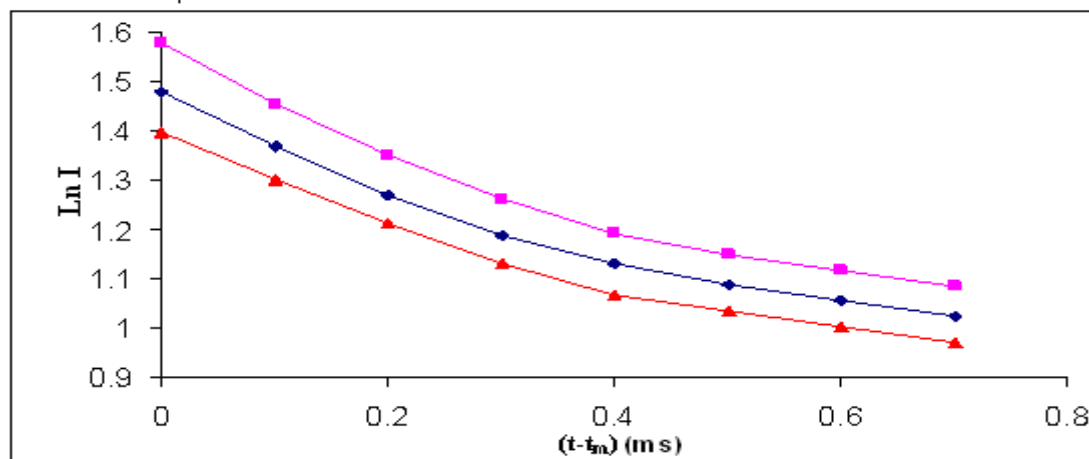


Fig.5 Plot of $\log I$ versus $(t-t_m)$.

Figure 5 shows the plot between the log of ML intensity I and $(t-t_m)$. When the ZnS:Mn nanoparticle is deformed impulsively by the impact of the load, then after t_m , initially the ML intensity decreases at a fast rate and then it decays at the slow rate. Infact, the decay time of the fast decay in ML is related to the decay time of the deformation rate of ZnS:Mn nanoparticles and the decay time of slow decrease in the ML intensity is related to the decay time of electrons from the shallow traps in which the thermal release of electron from the shallow traps takes place subsequently the recombination of such electrons with the holes may cause release of energy which may be transferred non radiatively to Mn^{2+} ions, whereby the Mn^{2+} ions may excite and its de-excitation may give rise to the light emission characteristics of the Mn^{2+} ions[43].

Table 1. Value of τ_1 and τ_2 for different values of height through which load is dropped.

Height	Sample	(τ_1) (ms)	(τ_2) (ms)
20cm	A1	1.07	3.1
30cm	A2	.954	3.11
40cm	A5	.874	3.08
45cm			

The elasto-mechanoluminescence[EML], plasto-mechanoluminescence[PML] and fracto-mechanoluminescence [FML] of II-VI semiconductors are known since long time. As EML occurs only in Mn doped II-VI semiconductors, the EML of ZnS:Mn has been attributed to the piezoelectric effect induced by elastic deformation near Mn centres. The PML which is observed in all II-VI semiconductors has been attributed to the electrostatic field produced near the charged dislocations. The FML may occur due to the piezoelectric effect as well as due to electrostatic field near the charged dislocations, however for the crystals of micrometer size and bigger size the moving dislocations are the origin of FML. In the case of nanoparticles dislocation segment is very small and hence the bending in the dislocation segment may not be significant to cause the appreciable interaction between the bending segment of dislocation and filled electron traps in the nanocrystals. It seems that FML in ZnS:Mn nanocrystals arises due to the piezoelectric field near the newly created surface of the nanocrystals. In the case of dislocation model, the ML intensity is directly proportional to the applied stress, however, the experimental results indicates that the total ML intensity is directly proportional to the square of the applied stress i.e. proportional to the height through which the load is dropped on the nanoparticles. On the other hand, the piezoelectric model of ML indicates that the piezoelectric field induced by deformation of ZnS:Mn nanoparticles is responsible for the ML excitation. In this case, the total ML intensity is directly proportional to the applied stress and the experimental results indicates that the total ML intensity is directly proportional to the square of the applied stress i.e. proportional to the height through which the load is dropped on the nanoparticles. Thus the present investigation indicates that the pizeoelectrification is responsible for the ML excitation of ZnS:Mn nanoparticles.

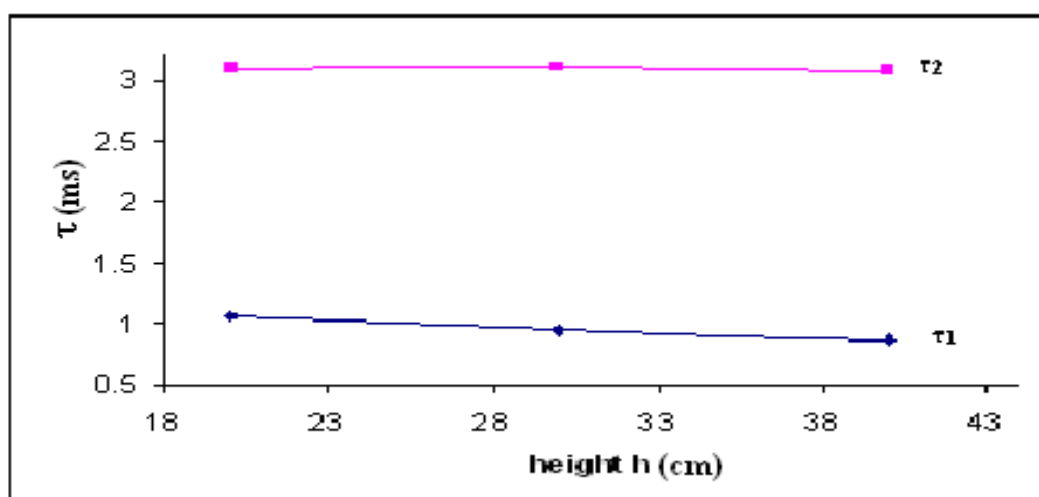


Fig. 6 Plot of graph τ verses height h .

Fig. 6 shows the dependence of τ_1 and τ_2 with respect to height through which the load is dropped on to the nanoparticles. Where τ_1 is the decay time of the rate of compression of the nanoparticles and τ_2 is the life time of electrons in the shallow traps. It is seen from the figure that τ_2 does not change with height, but τ_1 decreases with the increase in the height.

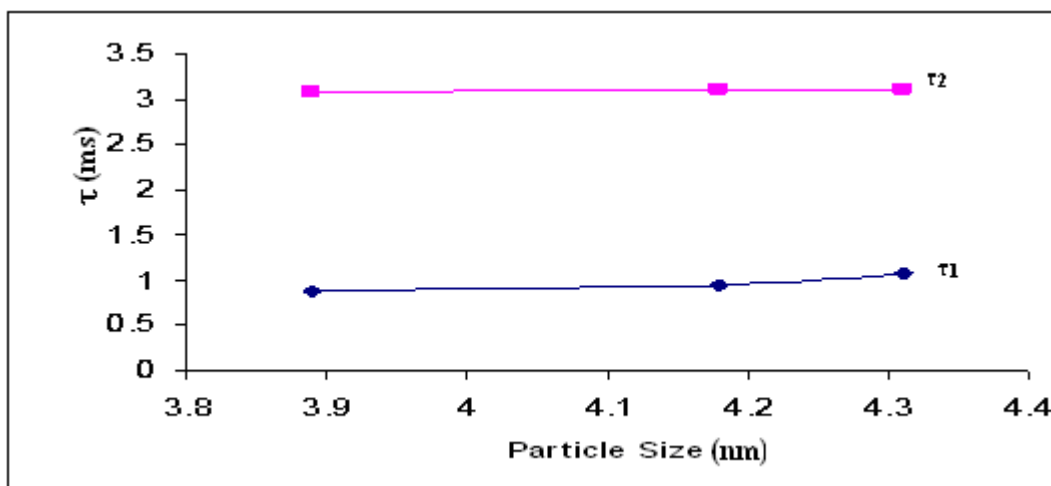


Fig. 7 plot of τ versus particle size.

Fig. 7 shows the dependence of τ_1 and τ_2 with the particle size. It is very clear from the figure that τ_1 and τ_2 do not show much difference for the different size of the nanoparticles.

5. Conclusion

The nanoparticles of ZnS:Mn were grown by chemical route in which mercaptoethanol was used as capping agent. The XRD and TEM pattern indicated the growths of the nanoparticles. The size of the nanocrystals were found to be 3-5 nm. The ML intensity of ZnS:Mn nanocrystal increases with increase in the mechanical stress. The ML in ZnS:Mn nanocrystals can be understood on the basis of the piezoelectrically-induced electron detrapping model, in which the local piezoelectric field near the Mn^{2+} centres reduces the trap-depth, and therefore, the detrapping of filled electron traps takes place, and subsequently the energy released non-radiatively during the electron-hole recombination excites the Mn^{2+} centres and de-excitation gives rise to the ML. Thus, the ML can be used for impact sensing.

Acknowledgement

All the samples were characterized at Inter University Consortium (IUC) Indore. The first author is very much thankful to Dr. R.J. Choudhry and Dr.N.P. Lalla of Inter University Consortium (IUC) Indore for providing XRD and TEM facility.

References

- [1] P.W. Cyr, M. Tzolov, M.A. Hines, I. Manners, E.H. Sargent, G.D. Scholes, Quantum dots in a metallopolymer host: studies of composites of polyferrocenes and CdSe nanocrystals, *J. Mater. Chem.* **13**, 2213 (2003).
- [2] H. Fendler, F.C. Meldrum, The colloid chemical approach to nanostructured materials, *Adv. Mater.* **7**, 607 (1995).
- [3] N. Lopez, T.V.W. Janssens, B.S. Clausen, Y. Xu, M. Mavrikakis, T. Bligaard, J.K. Nørskov, On the origin of the catalytic activity of gold nanoparticles for low-temperature CO oxidation, *J. Catal.* **223**, 232 (2004).
- [4] A.P. Alivisatos, Semiconductor clusters, nanocrystals, and quantum dots, *Science* **271**, 933 (1996).

- [5] T. Ahmadi, Z.L. Wang, T.C. Green, A. Henglein, M.A. El-Sayed, Shape-controlled synthesis of colloidal platinum nanoparticles, *Science* **272**, 1924 (1996).
- [6] D. Yelin, D. Oron, S. Thiberge, E. Moses, Y. Silberberg, Multiphoton plasmonresonance microscopy, *Opt. Express* **11**, 1385 (2003).
- [7] J. Walton, *Adv. Phys.* **26**, 887 (1977).
- [8] Y. Enomoto, H. Hashimoto, and K. Kikuchi, *Philos. Mag. A* **74**, 1299 (1996); K. Nakayama and H. Hashimoto, *Wear* **147**, 355 (1991).
- [9] G. E. Hardy, W. C. Kaska, B. P. Chandra, and J. I. Zink, *J. Am. Chem. Soc.* **103**, 1074 (1981).
- [10] G. Alzetta, I. Chudacek and R. Scarmozzino, *Phys. Status Solidi A* **1**, 775 (1971).
- [11] B. P. Chandra, *Radiat. Eff. Defects Solids* **138**, 119 (1996).
- [12] A. V. Shuldiner and V. A. Zakrevskii, *Radiat. Prot. Dosim.* **65**, 113(1996).
- [13] B. P. Chandra, M. S. Khan, S. R. Singh, and M. H. Ansari, *Cryst. Res. Technol.* **31**, 495 (1996).
- [14] J. I. Zink and B. P. Chandra, *J. Phys. Chem.* **86**, 5 (1982).
- [15] L. M. Sweeting, M. L. Cashel, and M. M. Rosenblatt, *J. Lumin.* **52**, 281(1992).
- [16] B.P. Chandra, J. I. Zink, *Phys. Review*, **B21**, 816 (1980).
- [17] C. N. Xu, T. Watanabe, M. Akiyama, X. G. Zheng, *Appl. Phys. Lett.* **74**, 1236 (1999).
- [18] I. Sage, L. Humerstone, I. Oswald, Lloyed, G. Bourhill, *Smart Mater. Struct.* **10**, 332 (2001).
- [19] C. N. Xu, X. G. Zheng, M. Akiyama, K. Nonaka, T. Watanabe, *Appl. Phys. Lett.* **76**, 179 (2000).
- [20] K. S. Sohn, S. Y. Seo, Y. N. Kwon, H. D. Park, *J. Am. Ceramic, Soc.* **85**, 712(2002).
- [21] J. S. Kim, Y. N. Kwon, N. Shin and K. S. Sohn, *Appl. Phys. Lett.* **90**, 241916 (2007).
- [22] A.A. Khosravi, M.Kundu, G.S.Shekhawat, R.R.Gupta, A.K.Sharma, P.D.Vyas, S.K.Kulkarni, *Appl. Phys. Lett.* **67**, 2506 (1995).
- [23] H. Y. Lu, S. Y. Chu, *J. Crystal Growth*, **265**, 476 (2004).
- [24] M. I. Molotskii, *Sov. Sci. Rev. B: Chem.* **13**, 1(1989).
- [25] A. J. Walton, *Adv. Physics* **26**, 887(1977).
- [26] K. Meyer, D. Obrikat and M. Rossberg, *Kristall. U Tech* **5** (1970); *ibid* **5**, 181.
- [27] C.N. Xu, *Encyclopedia of Smart Materials*, Vol. 1, edited by Schwarz M., John Willey & Sons, Inc.(2002) , pp190-201.
- [28] Y. Zia, M. Yei and W. Jia, *Optical Materials*, **28**, 974 (2006).
- [29] J. S. Kim, K. Kibble, Y. N. Kwon, K. S. Sohn, *Optics Letters* **34**, 1915(2009).
- [30] B. P. Chandra, S.K. Mahobia, P. Jha, R.K. Kuraria S.R. Kuraria R.N. Baghel, S. Thaker J. *Lum.* **128**, 2038(2008)
- [31] B.P.Chandra, *J. Lum.* **128**, 1217(2008).
- [32] B. P.Chandra, S. K.Mahobia, R. K. Kuraria, V. Choudhary, *Indian J.Eng. & Materials Sciences*, **14**, 443(2007).
- [33] B. P.Chandra, R. N.Baghel, A. K. Luka, T. R. Sanodiya, R. K. Kuraria, S. R. Kuriaria, *J. Lum.* **129**, 760(2009).
- [34] B. P. Chandra, in *Luminescence of Solids*, edited by Vij, D.R., Plenum Press, New York, pp 361-389. (1998).
- [35] S. I. Bredikhin, S. Z. Shmurak, *Sov. Phys. JETP* **49**, 520 (1979).
- [36] L. Grmela, R. Macku, P. Tomanek, *J. Microscopy* **229**, 275 (2008).
- [37] V. Wood, J. E. Halpert, M. J. Panzer, M. G. Bawend, V. Bulonic, *Nano Letters*, **2367**(2009).
- [38] K. Manzoor, S. R. Vadera, N. Kumar, T. R. N. Kutty, *Appl. Phys. Let.* **84**,284(2004).
- [39] J. F. Suyver, S. F. Wuister, J. J. Kelly, Meijrink, *Nano Letters*, **1**, 429 (2001).
- [40] S. Mahamuni, A.A. Khosravi, M.Kundu, A. Kshirsagar, A. Bedekar, D.B. Avasare, P.Singh, S.K. Kulkarni, *J. Appl. Phys.*,**73**, 5237, (1993).
- [41] Guinier, A. *X-ray Diffraction*, Freeman, San Francisco (1963).
- [42] C. N. Xu, M. Akiyama and T. Watanabe *IEEE Trans.UFFC*.**45(4)**:1065 (1998).
- [43] B.P. Chandra, C.N. Xu, H. Yamada, X.G. Zheng, *J. Lumin.* **130**, 442 (2010).